Pressure and energy behavior of the Gaussian core model fluid under shear

Alauddin Ahmed,[1] Peter Mausbach,[2] and Richard J. Sadus[1]

[1]*Centre for Molecular Simulation, Swinburne University of Technology, P.O. Box 218, Hawthorn, Victoria 3122, Australia*
[2]*Cologne University of Applied Sciences, 50679 Cologne, Germany*

The pressure and energy behavior of the Gaussian core model (GCM) fluid as a function of strain-rate are obtained from nonequilibrium molecular dynamics simulations for a wide range of thermodynamic state points. An analytical dependence of pressure on strain-rate is observed which is in agreement with a Taylor series expansion of pressure in terms of the strain-rate tensor. In contrast, the energy as a function of strain rate is found to be dependent on temperature and density. The different behavior of pressure and energy contradicts mode-coupling theory, which requires the same variation of pressure and energy with respect to the strain-rate. The results for the GCM fluid do not support the hypothesis that the strain-rate exponent for both pressure and energy can be universally represented by a simple linear function of temperature and density.

I. INTRODUCTION

The leading non-Newtonian behavior of a fluid is a subject of longstanding scientific interest [1–11]. The fundamental observation of long-time tails [1] is the subject of many theoretical [2–5] and simulation [6–11] studies. One of the main predictions is the nonanalytical behavior of the hydrostatic pressure as a function of strain-rate ($\dot{\gamma}$). Mode-coupling theory predicts a $\dot{\gamma}^{3/2}$ dependency of pressure, which has been confirmed by molecular simulations [6,7] for a Lennard-Jones fluid at its triple point. Phenomenological relationships [6–11] for hydrostatic pressure and energy as a function of strain-rate have been proposed using nonequilibrium molecular dynamics (NEMD) data. Although NEMD data and the relationships are in general agreement, there is a discrepancy of more than 2 orders of magnitude in the values of the coefficients for the non-linear contributions.

It has been argued [7] that this difference is a consequence of the high strain-rates used in molecular simulation. In contrast to the relationships proposed by Evans and Hanley [6], extended irreversible thermodynamics (EIT) [12–14] predicts the dependence of pressure and energy on strain-rate is analytical, i.e., both quantities vary as $\dot{\gamma}^2$. To test this apparent contradiction Nettleton [15] introduced the volume fraction of locally dilated spherical regions as an additional state variable and studied the transition from $\dot{\gamma}^2$ to $\dot{\gamma}^{3/2}$ behavior. Nettleton observed a bifurcation in the asymptotic solution with a $\dot{\gamma}^{3/2}$ dependence for pressure and energy at high strain rates. Similar disagreements with mode-coupling theory are also observed in equilibrium molecular dynamics (EMD) simulations [16] and in simulated cyclic compression [17]. Matin *et al.* [18] found that the $\dot{\gamma}^{3/2}$ variation of pressure and energy was only observed in the vicinity of the triple point. The 3/2 exponent was also questioned by NEMD results for the pressure of shearing dense fluids away from the triple point [19,20]. Ge *et al.* [21] determined that the power law exponent varies continuously between $\sim$1.2 and $\sim$2 as a linear function of density and temperature. The same linear relationship also applies to the Barker-Fisher-Watts fluid [22] suggesting it is independent of the specifics of the interaction potential [23]. Subsequently, Desgranges and Delhommelle

[24] demonstrated that the coefficients of this linear relationship are also the same for a realistic many-body potential. This result is consistent with the thermodynamic fluctuation theory, which requires that the shear dilatancy exponent must be less [25] than 2.

Previous theoretical and simulation studies on the non-Newtonian behavior of fluids have largely focused on unbounded potentials. Recently, considerable interest has been focused on bounded potentials, such as the Gaussian core model (GCM), because of their usefulness in soft condensed matter physics [26]. The GCM fluid qualitatively imitates the anomalies of complex molecular fluids and their solutions. It exhibits density [27] and structural [29] anomalies as well as other waterlike anomalies [28] associated with re-entrant melting behavior. It has been observed [30,31] that transport properties like the self-diffusion coefficient and the shear viscosity of the GCM fluid also show anomalous behavior. For example, at high densities where penetration of GCM particles becomes dominant, shear viscosity increases with increasing temperature. This is consistent with the experimentally observed behavior of cationic surfactant (wormlike micellar) solutions [32]. It appears that the GCM can be used to model the *effective* interactions of micellar aggregates of ionic surfactants suggested by Baeurle *et al.* [33].

In view of the anomalous strain-rate dependent viscosity behavior [30], it is of considerable interest to also study the pressure and energy behavior of the GCM fluid as a function of strain-rate. Therefore, we present a comprehensive analysis of extensive NEMD simulation data and compare them to both existing theoretical and phenomenological models. We report relationships for pressure and energy for the GCM fluid as a function of strain-rate and we demonstrate how the model parameters vary with temperature and density.

II. SIMULATION DETAILS

The isothermal isochoric NEMD simulations were performed on a homogenous fluid of 4000 particles interacting via a GCM potential of the form:

$$u(r) = \varepsilon \, \exp\!\left[-\left(\frac{r}{\sigma}\right)^2\right], \qquad (1)$$

where ε and σ are the height and width of the potential. The sllod [34] equations of motion were integrated using a five-value Gear predictor-corrector scheme [35]. Lees-Edwards periodic boundary conditions [36] and a Gaussian thermostat [37] were used. The normal conventions were used for the reduced density ($\rho^* = \rho\sigma^3$), temperature ($T^* = kT/\varepsilon$), energy ($E^* = E/\varepsilon$), pressure ($p^* = p\sigma^3/\varepsilon$), viscosity ($\eta^* = \eta\sigma^2/\sqrt{m\varepsilon}$), strain-rate ($\dot{\gamma}^* = \dot{\gamma}\sqrt{m\sigma^2/\varepsilon}$), and time ($\tau^* = \tau\sqrt{\varepsilon/m\sigma^2}$). All quantities quoted in this work are in terms of these reduced quantities and the asterisk superscript will be omitted in the rest of the paper.

The simulations covered five isochors of densities $\rho = 0.1$, 0.2, 0.3, 0.4, and 1.0, temperatures ranging from $T = 0.015$ to 3.0. The strain-rates used in this study were terminated at 'safe' values [30] to avoid string phases. Further simulation details are discussed elsewhere [30]. It has been previously shown [25] that an analytical expansion for the pressure in the asymptotic limit of zero shear does not exist. At very high temperatures pressure and energy variations of the GCM fluid are sensitive to the low strain-rates. Therefore in our study we have carefully avoided the pressure and energy variation for $\dot{\gamma} \rightarrow 0$ at high temperatures.

III. STRAIN-RATE DEPENDENCE OF PRESSURE AND ENERGY

To analyze the NEMD data for the pressure and energy behavior of the GCM fluid as a function of strain-rate, we used the following pair of equations proposed by Evans and Hanley [6]:

$$\left.\begin{array}{l} p(\rho, T, \dot{\gamma}) = p_0(\rho, T) + p_{\dot{\gamma}}(\rho, T)\dot{\gamma}^\alpha \\ E(\rho, T, \dot{\gamma}) = E_0(\rho, T) + E_{\dot{\gamma}}(\rho, T)\dot{\gamma}^\alpha \end{array}\right\}, \qquad (2)$$

where the 0 and $\dot{\gamma}$ subscripts denote equilibrium and shearing contributions respectively. In this work, we tested three different hypotheses for the α exponent, corresponding to mode-coupling theory (MCT), analytical behavior (AB), and a density-temperature functional behavior (ρTF), i.e.,

$$\alpha = \begin{cases} 3/2 & \text{MCT} \\ 2 & \text{AB} \\ f(\rho, T) & \rho\text{TF} \end{cases} \qquad (3)$$

Several workers [2,38–42] have demonstrated that Lennard-Jones simulation data at the triple point are in very good agreement with the MCT hypothesis. In contrast, Ge *et al.* [21] showed that away from the triple point, and for a wide range of thermodynamic state points, the power law exponent is not independent of density and temperature. They proposed a ρTF description of the α exponent. Using a Taylor series expansion Ge *et al.* [20] calculated that the leading term of pressure and energy must vary as $\dot{\gamma}^2$ if the pressure is analytical in powers of the strain rate. This result is also predicted by EIT. We are not aware of any simple liquids that exhibit AB in pressure and energy. Ge *et al.* [21]
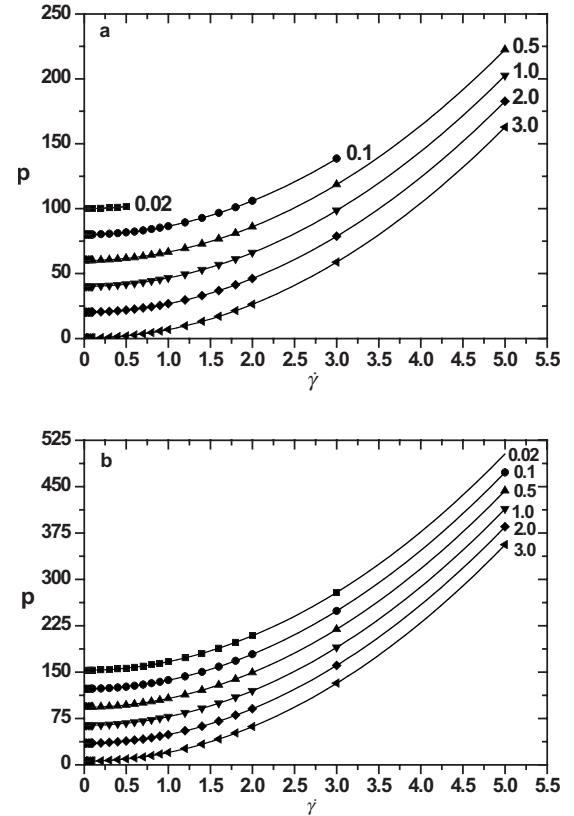
FIG. 1. Pressure as a function of strain-rate at densities of (a) $\rho = 0.1$ and (b) $\rho = 1.0$ for different temperatures $T = 0.002$ (■), 0.1 (●), 0.5 (▲), 1.0 (▼), 2.0 (◆) and 3.0 (◄) (data from simulations). ρTF fits are shown as thin continuous lines. The $T = 0.02$, 0.1, 0.5, 1.0, and 2.0 pressure isotherms are shifted by 100, 80, 60, 40, and 20 in Fig. 1(a) and by 150, 120, 90, 60, and 30 in Fig. 1(b), respectively, in order to avoid overlap.

determined a simple linear ρTF for the Lennard Jones. Conducting NEMD simulations on liquid metals Desgranges and Delhommelle [24] conjectured that the linear form of α as a function of temperature and density, which is a special case of ρTF [Eq. (3)] with a specified set of coefficients, could be used universally for all atomic liquids.

IV. RESULTS AND DISCUSSION

A. Strain-rate dependent pressure behavior

To examine the consistency of the strain-rate dependent pressure we do not assume any value of the scaling exponent (e.g., 3/2 or 2) or linear ρTF behavior, but determine its value *a posteriori* via a least-squares fit of the pressure as a function of strain-rate (ρTF). We then extract the value of α for each (ρ, T) state point and compare the behavior with the MCT and AB hypotheses. Typical pressure fits as a function of strain-rate are shown in Fig. 1 for densities of $\rho = 0.1$ (a) and $\rho = 1.0$ (b) at temperatures ranging from $T = 0.02$ to 3.0. The agreement between simulated results and the power-law fit is very good which allows an accurate determination of the model parameters.

The state point dependency of the fitting parameters is shown in Fig. 2. Figure 2(a) shows the equilibrium pressure
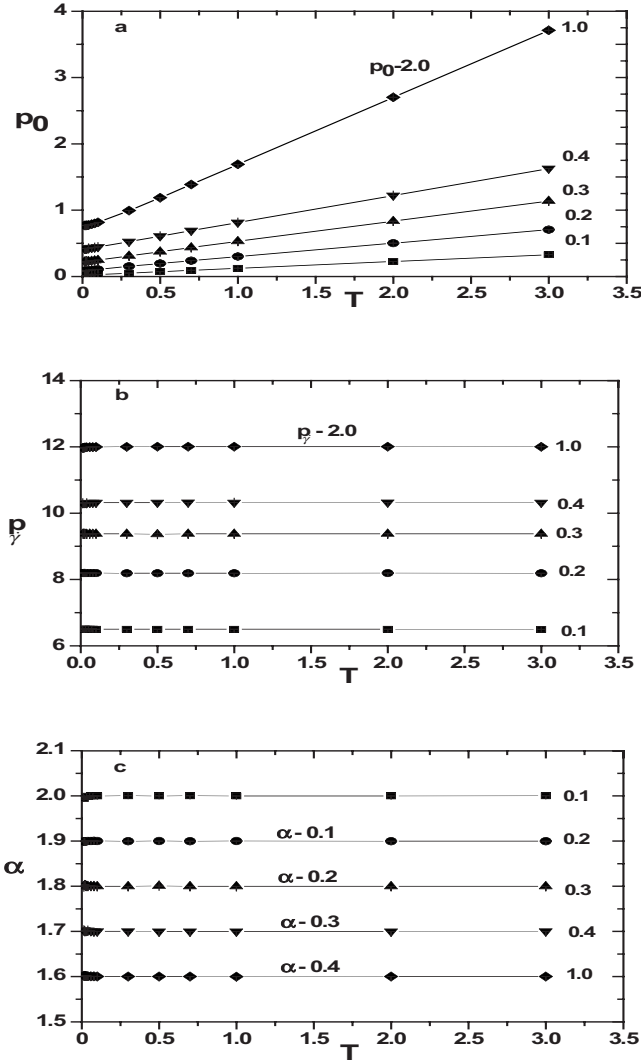
FIG. 2. Parameters (a) p_0, (b) $p_{\dot{\gamma}}$, and (c) α of the ρTF fit as a function of temperature for densities $\rho=0.1$ (■), 0.2 (●), 0.3 (▲), 0.4 (▼), and 1.0 (♦). Data obtained from the ρTF fit with the pressure data from simulations as a function of strain-rate. In Fig. 2(a) and 2(b) the pressure isochor for $\rho=1.0$ is shifted by -2 and in Fig. 2(c) the α isochors are shifted by -0.1 each starting at $\rho=0.2$ in order to avoid overlap.

(p_0) as a function of temperature for five different densities. To avoid a large pressure scale the p_0 isochor for $\rho=1.0$ is shifted by -2. At low temperatures and for densities $\rho>0.2$ the slope of the pressure exhibits a weak minimum (not resolved on the scale of the figure), which corresponds to the well-known density maximum of the GCM at constant pressure [27,28]. Apart from this anomaly the pressure isochors grow monotonically with increasing temperature for all densities.

The strain-rate dependent ($p_{\dot{\gamma}}$) term as a function of temperature is shown in Fig. 2(b) for five densities. Again, the pressure isochor for $\rho=1.0$ is shifted by -2. The $p_{\dot{\gamma}}$ values show only a weak temperature dependency and grow monotonically with increasing density. In Fig. 2(c) we illustrate α as a function of temperature for five different densities. To avoid overlaps the α isochors are shifted by -0.1
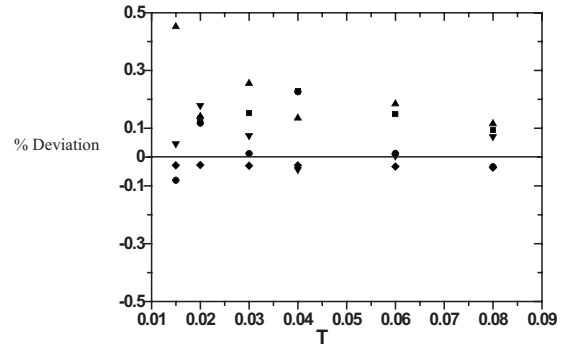
FIG. 3. Comparison of the relative percentage difference of the zero-shear pressure obtained from the ρTF fit with EMD calculations (Ref. [31]) as a function of temperature and densities of $\rho=0.1$ (■), 0.2 (●), 0.3 (▲), 0.4 (▼), and 1.0 (♦).

each starting at $\rho=0.2$. Figure 2(c) clearly indicates that α is completely independent on the state point with a value of approximately 2, which strongly supports the AB hypothesis and clearly contradicts the MCT hypothesis.

It is of interest to compare p_0 values obtained from the ρTF hypothesis with equilibrium values obtained elsewhere [31] from EMD simulations. Figure 3 compares EMD and ρTF p_0 values along isochors at $\rho=0.1$, 0.2, 0.3, 0.4 and 1.0 as a function of temperature. The comparison indicates that the discrepancies between the ρTF p_0 values and the EMD calculations are typically less than 0.3%.

To quantify the quality of agreement we also fitted the simulation data using AB and compared the percentage average absolute deviations (%ADD). These data are summarized in Table I; in all cases the squared-correlation function was 1. In Fig. 4 we show the deviations of the hydrostatic pressures obtained from simulation with hydrostatic pressures calculated using AB for two state points ($\rho=0.1$, $T=0.015$) and ($\rho=1.0$, $T=3.0$). The deviations fluctuate around zero and the extent of the longitudinal and lateral variation of the data fluctuates within a $\pm0.04\%$ range as a function of strain-rate. The plot also indicates a more accurate fit in the high strain-rate region. The % AAD values in

TABLE I. Percentage average absolute deviation (% AAD) values of AB and ρTF fits with simulation pressure data obtained in this work for five densities and two extremum temperatures of each density.

ρ	T	AB	ρTF
0.1	0.015	0.011	0.002
	3.0	0.123	0.11
0.2	0.015	0.006	0.001
	3.0	0.258	0.247
0.3	0.015	0.034	0.002
	3.0	0.636	0.523
0.4	0.015	0.186	0.02
	3.0	0.233	0.227
1.0	0.015	0.682	0.04
	3.0	0.334	0.327
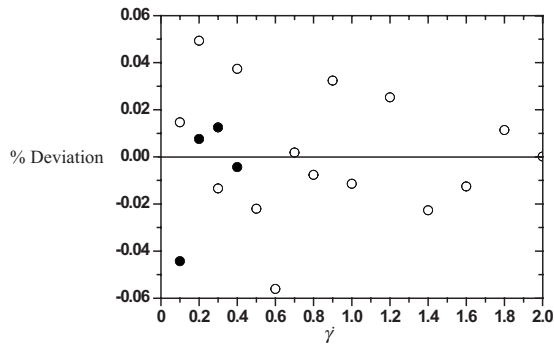
FIG. 4. Comparison of the relative percentage difference of hydrostatic pressures obtained from simulation with the hydrostatic pressures calculated from the AB fit as a function of strain-rate for the state points ($\rho=0.1$, $T=0.015$) (●) and ($\rho=1.0$, $T=3.0$) (○).

Table I and the deviations of pressure in Fig. 4 suggest that either the AB or ρTF hypotheses can be used to accurately fit the data for all strain-rates. However, as the AB fit requires only two parameters, it should be preferred to the ρTF fit. In contrast, the MCT hypothesis does not work for the GCM fluid. These considerations indicate that the pressure variation of the GCM fluid under shear behaves analytically.

B. Strain-rate dependent energy behavior

Following the same procedure as for the pressure, we determined the fitting parameters of the strain-rate dependent potential energy per particle *a posteriori* via least-squares fits using the ρTF hypothesis. Typical fits of the potential energy as a function of strain-rate are shown in Fig. 5 for densities of of (a) $\rho=0.1$ and (b) $\rho=0.4$ at temperatures ranging from T =0.015 to 0.08. Unlike the pressure data, the strain-rate profiles of the potential energy do not display simple power-law behavior for $T>0.1$ (not shown in Fig. 5), which suggests that Eq. (2) is not valid for high temperatures. Therefore, we only analyzed the strain-rate dependent potential energy up to $T=0.1$ for $\rho=0.1$ to 0.4 and up to $T=0.06$ at $\rho=1.0$. As is shown in Fig. 5, in these ranges we find good agreement between simulation results and the ρTF.

The state point dependencies of the fitting parameters are shown in Figs. 6 and 7. Figure 6(a) shows the equilibrium energy E_0 as a function of temperature for five different densities. The E_0 isochor for $\rho=1.0$ is shifted by -1.5. The zero-strain energy E_0 grows monotonically with increasing density [Fig. 7(a)] and temperature [Fig. 6(a)] where the effect of temperature is weaker than the effect of density. The strain-rate dependent contribution ($E_{\dot\gamma}$) is shown in Fig. 6(b) as a function of temperature for different constant densities. Figure 7(b) shows $E_{\dot\gamma}$ as a function of density for different constant temperatures. Up to a density of approximately 0.23, $E_{\dot\gamma}$ increases with increasing density at constant temperature and decreases with increasing temperature at constant density. This behavior is consistent with the behavior reported for the Lennard-Jones fluid. For densities greater than 0.23, $E_{\dot\gamma}$ decreases with increasing density at constant temperature showing an anomalous density dependency in this region.
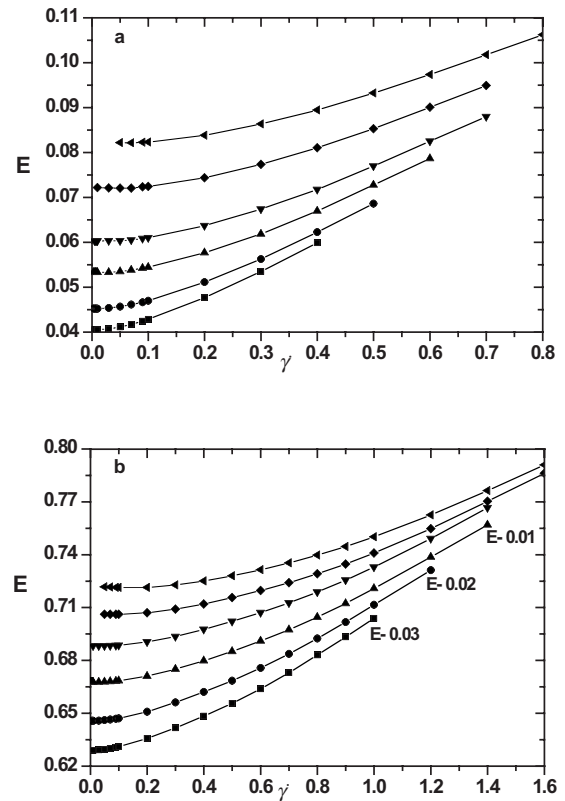
FIG. 5. Potential energy per particle as a function of strain-rate at densities of (a) $\rho=0.1$ and (b) $\rho=0.4$ for different temperatures $T=0.015$ (■), 0.02 (●), 0.03 (▲), 0.04 (▼), 0.06 (♦), and 0.08 (◄) (data from simulations). The ρTF fits are shown as thin continuous lines. The energy isotherms in Fig. 5(b) for temperatures $T=0.015$, 0.02 and 0.03 are shifted by -0.03, -0.02, and -0.01, respectively, in order to avoid overlaps.

In Fig. 6(c), we illustrate the α exponent for the potential energy as a function of temperature for different constant densities and in Fig. 7(c) as a function of density for different constant temperatures. Up to a density of approximately 0.23, α decreases with increasing density at constant temperature and increases with increasing temperature at constant density. The temperature dependency of α is approximately linear [Fig. 6(c)] except for $\rho=1.0$. Again, this behavior is consistent with that of a Lennard-Jones fluid. For densities greater than 0.23, α increases with increasing density at constant temperature showing behavior similar to the $E_{\dot\gamma}$ density dependency in this region. It is of interest to note that at a density of 0.23 many equilibrium properties of the GCM change also from normal to anomalous behavior [28]. In the nonequilibrium sheared fluid state the energy behavior of the GCM characterized by the shearing parameters $E_{\dot\gamma}$ and α reflects the equilibrium behavior of the system.

Similar to the pressure data, we compared values of E_0 obtained from the ρTF fit with equilibrium values obtained from EMD simulations [31] at constant density and different temperatures (Fig. 8). The comparison indicates that the discrepancies between E_0 extracted from the fit and EMD calculations are typically less than 0.2% and in general they are higher than the EMD values.
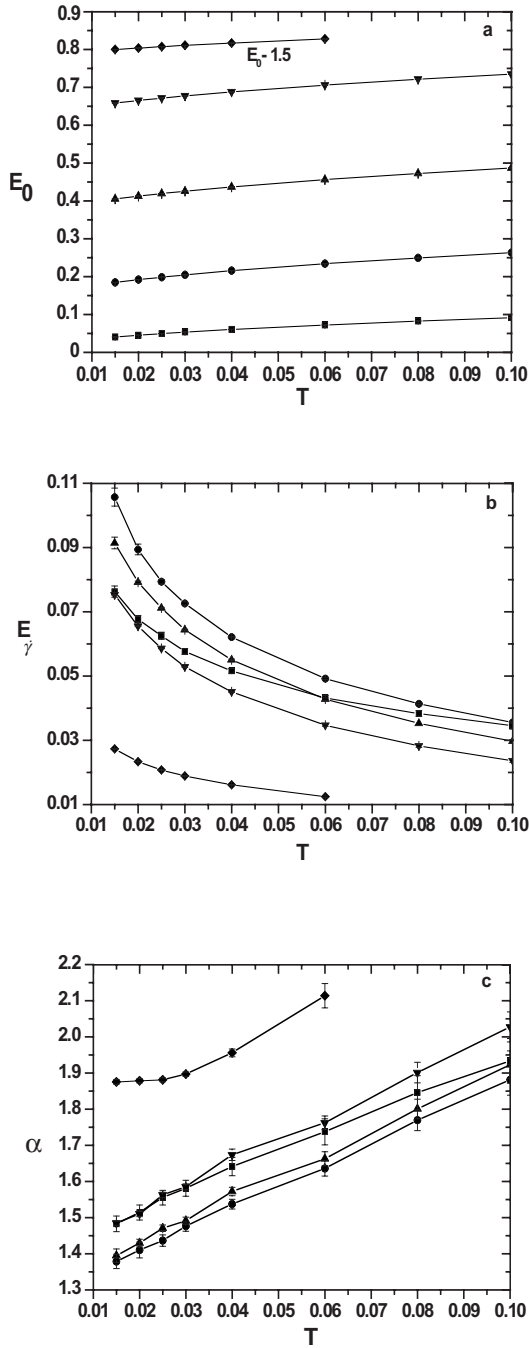
FIG. 6. Values of (a) E_0, (b) $E_{\dot{\gamma}}$, and (c) α as functions of temperature obtained from the simulation data via a least-squares ρTF fit for densities $\rho=0.1$ (■), 0.2(●), 0.3 (▲), 0.4 (▼), and 1.0 (♦). In Fig. 6(a) the E_0 isochor for $\rho=1.0$ is shifted by -1.5.

FIG. 7. Values of (a) E_0, (b) $E_{\dot{\gamma}}$, and (c) α as functions of density obtained from the simulation data via a least-squares ρTF fit for temperatures $T=0.015$ (■), 0.02 (●), 0.025 (▲), 0.03 (▼), 0.04 (♦), 0.06 (◄), 0.08, (►) and 0.1(●).

The strong state point dependency of α clearly contradicts both the MCT and AB hypotheses. Unlike the pressure, the data points of our simulations support the general ρTF hypothesis of Eq. (3) but clearly contradict the linear ρTF behavior of Ge *et al.* [21] However, for increasing temperature and decreasing density the error bars for α increase [Figs. 6 and 7(c)]. To quantify the quality of the ρTF fit we calculated the % relative deviation of the potential energy per particle as a function of strain-rate. The percentage deviation in Fig. 9 show typical deviations of the model for two

state points ($\rho=0.1$, $T=0.015$) and ($\rho=0.4$, $T=0.1$), which fluctuate around zero. The extent of the longitudinal and lateral variation of the data indicates that for the state point ($\rho=0.4$, $T=0.1$) the calculations systematically deviate from the simulation results at low strain-rates but attain improved agreement at high strain-rates. Nonetheless, the % relative deviations in Fig. 9 indicate that the ρTF fit provides a good overall description of the simulation data and as such provide evidence of the nonanalyticity of the potential energy variation of the GCM fluid under shear.
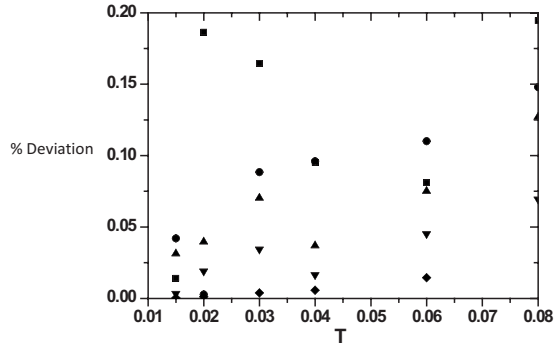
FIG. 8. Comparison of the relative percentage difference of the zero-shear potential energy per particle E_0 obtained from a ρTF fit with EMD calculations (Ref. [31]) as a function of temperature and densities of $\rho=0.1$ (■), 0.2 (●), 0.3 (▲), 0.4 (▼), and 1.0 (♦).

C. Comparison with theoretical predictions

In this study, we found that a number of well known theoretical predictions are violated by the pressure and potential energy behavior of the GCM fluid under shear. The mode-coupling theory results of Kawasaki *et al.* [2,4] and Ernst *et al.* [5] and thermodynamic fluctuation theory of Evans *et al.* [25,42] suggest that both pressure and energy are nonanalytical functions of strain-rate. Contrary to this we found that the pressure of the GCM fluid varies analytically independent of the state point. This analytical dependence is consistent with a Taylor series expansion of hydrostatic pressure as powers of the strain-rate tensors [20]. Another interesting prediction of mode-coupling theory is that the pressure and energy will follow the same power law behavior. Since the pressure of the GCM fluid is analytical and energy is state point dependent the behavior of these quantities far from equilibrium clearly contradicts the mode-coupling prediction. In addition, EIT [12–14] predicts that both pressure and energy have a $\dot{\gamma}^2$ dependency. This theoretical prediction is violated by the energy behavior of the GCM fluid. We are not aware of any other simple fluid that follows two different power law models for pressure and energy. The universal scaling behavior [21,24] is a linear relationship between ρ and T and contains a specific set of coefficients. It was obtained [21] from a linear regression of both pressure and energy exponents as function of ρ and T. In contrast, for the GCM fluid, linear regression fails to correlate both the pressure and energy ex-
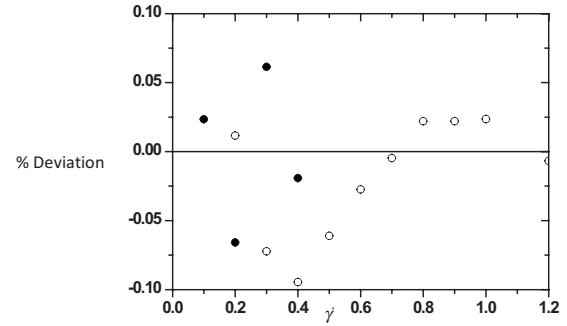
FIG. 9. Comparison of the relative percentage difference of potential energies per particle obtained from simulation with the energies calculated from an ρTF fit as a function of strain-rate for the state points ($\rho=0.1$, $T=0.015$) (●) and ($\rho=0.4$, $T=0.1$) (○).

ponents. Therefore, the hypothesis that the state point dependent functional form of the power-law exponent α can be expressed universally as a simple linear function of temperature and density for both pressure and energy [21,24] is also violated by the GCM fluid because of the strong nonlinear density dependence of the energy exponent. Note that this behavior does not contradict the validity of the general ρTF form according to Eq. (3).

V. CONCLUSIONS

Extensive NEMD simulation data were examined to obtain the accurate pressure and energy behavior of the GCM fluid under shear. We assumed that the strain-rate dependent pressure and energy observe simple power-law dependence. We found that the pressure is analytic in strain-rate while the energy shows a strong state point dependency. The two different power laws for pressure and energy contradict the original mode-coupling prediction, which suggests the same power-law exponent of 3/2. The results for the GCM fluid contradict the hypothesis that the strain-rate exponent for both pressure and energy can universally be represented by a simple linear function of temperature and density.

ACKNOWLEDGMENTS

[1] B. J. Alder, D. M. Gass, and T. E. Wainwright, J. Chem. Phys. **53**, 3813 (1970).

[2] K. Kawasaki and J. D. Gunton, Phys. Rev. A **8**, 2048 (1973).

[3] Y. Pomeau and Résibois, Phys. Rep. **19**, 63(1975).

[4] T. Yamada and K. Kawasaki, Prog. Theor. Phys. **53**, 111 (1975).

[5] M. H. Ernst, B. Cichocki, J. R. Dorfman, J. Sharma, and H. van Beijeren, J. Stat. Phys. **18**, 237 (1978).

[6] D. J. Evans and H. J. M. Hanley, Phys. Lett. A **79**, 178 (1980); Phys. Lett. A **80**, 175 (1980).

[7] D. J. Evans, Phys. Rev. A **23**, 1988 (1981).

[8] H. J. M. Hanley and D. J. Evans, J. Chem. Phys. **76**, 3225 (1982).

[9] D. J. Evans, J. Chem. Phys. **78**, 3297 (1983).

[10] D. J. Evans, H. J. M. Hanley, and S. Hess, Phys. Today **37**, 26 (1984).

[11] K. D. Romig, Jr., and H. J. M. Hanley, Int. J. Thermophys. **7**, 877 (1986).

[12] D. Jou, J. Casas-Vázquez, and G. Lebon, *Extended Irreversible Thermodynamics*, 4th ed. (Springer, New York, 2010).

[13] C. Perez-Garcia and D. Jou, Phys. Lett. A **95**, 23 (1983).

[14] M. Grmela, Phys. Lett. A **120**, 276 (1987).

[15] R. E. Nettleton, J. Non-Equilib. Thermodyn. **12**, 273 (1987).

[16] J. Erpenbeck and W. W. Wood, J. Stat. Phys. **24**, 455 (1981).

[17] W. G. Hoover, D. J. Evans, R. B. Hickman, A. J. C. Ladd, W. T. Ashurst, and B. Moran, Phys. Rev. A **22**, 1690 (1980).

[18] M. Matin, P. J. Daivis, and B. D. Todd, J. Chem. Phys. **113**, 9122 (2000).

[19] G. Marcelli, B. D. Todd, and R. J. Sadus, Phys. Rev. E **63**, 021204 (2001).

[20] J. Ge, G. Marcelli, B. D. Todd, and R. J. Sadus, Phys. Rev. E **64**, 021201 (2001); **65**, 069901(E) (2002).

[21] J. Ge, B. D. Todd, G. Wu, and R. J. Sadus, Phys. Rev. E **67**, 061201 (2003).

[22] J. A. Barker, R. A. Fisher, and R. O. Watts, Mol. Phys. **21**, 657 (1971).

[23] J. Ge, Ph.D. thesis, Swinburne University of Technology, 2004.

[24] C. Desgranges and J. Delhommelle, Phys. Rev. E **79**, 052201 (2009).

[25] D. J. Evans and H. J. M. Hanley, Physica A **108**, 567 (1981).

[26] C. N. Likos, Phys. Rep. **348**, 267 (2001).

[27] F. H. Stillinger and D. K. Stillinger, Physica A **244**, 358 (1997).

[28] P. Mausbach and H. O. May, Fluid Phase Equilib. **249**, 17 (2006).

[29] W. P. Krekelberg, T. Kumar, J. Mittal, J. R. Errington, and T. M. Truskett, Phys. Rev. E **79**, 031203 (2009).

[30] A. Ahmed, P. Mausbach, and R. J. Sadus, J. Chem. Phys. **131**, 224511 (2009).

[31] P. Mausbach and H.-O. May, Z. Phys. Chem. **223**, 1035 (2009).

[32] G. C. Kalur, B. D. Frounfelker, B. H. Cipriano, A. I. Norman, and S. R. Raghavan, Langmuir **21**, 10998 (2005).

[33] S. A. Baeurle and J. Kroener, J. Math. Chem. **36**, 409 (2004).

[34] D. J. Evans and G. P. Morriss, *Statistical Mechanics of Non-equilibrium Liquids*, 2nd ed. (Academic, London, 2008).

[35] C. W. Gear, *Numerical Initial Value Problems in Ordinary Differential Equations* (Prentice-Hall, Englewood Cliffs, NJ, 1971).

[36] R. J. Sadus, *Molecular Simulation of Fluids: Theory, Algorithms, and Object-Orientation* (Elsevier, Amsterdam, 1999).

[37] D. J. Evans, W. G. Hoover, B. H. Failor, B. Moran, and A. J. C. Ladd, Phys. Rev. A **28**, 1016 (1983).

[38] D. J. Evans, G. P. Morris, and L. M. Hood, Mol. Phys. **68**, 637 (1989).

[39] D. J. Evans and S. Sarman, Phys. Rev. E **48**, 65 (1993).

[40] D. P. Hansen and D. J. Evans, Mol. Simul. **13**, 375 (1994).

[41] R. Bhupathiraju, P. T. Cummings, and H. D. Cochran, Mol. Phys. **88**, 1665 (1996).

[42] K. P. Travis, D. J. Searles, and D. J. Evans, Mol. Phys. **95**, 195 (1998).